UCRL 3435

UNIVERSITY OF CALIFORNIA

Radiation Laboratory

TWO-WEEK LOAN COPY

This is a Library Circulating Copy which may be borrowed for two weeks. For a personal retention copy, call Tech. Info. Division, Ext. 5545

BERKELEY, CALIFORNIA

DISCLAIMER

This document was prepared as an account of work sponsored by the United States Government. While this document is believed to contain correct information, neither the United States Government nor any agency thereof, nor the Regents of the University of California, nor any of their employees, makes any warranty, express or implied, or assumes any legal responsibility for the accuracy, completeness, or usefulness of any information, apparatus, product, or process disclosed, or represents that its use would not infringe privately owned rights. Reference herein to any specific commercial product, process, or service by its trade name, trademark, manufacturer, or otherwise, does not necessarily constitute or imply its endorsement, recommendation, or favoring by the United States Government or any agency thereof, or the Regents of the University of California. The views and opinions of authors expressed herein do not necessarily state or reflect those of the United States Government or any agency thereof or the Regents of the University of California.

UCRL-3435

UNIVERSITY OF CALIFORNIA
Radiation Laboratory
Berkeley, California

Contract No. W-7405-eng-48

THE SPIN OF NEON-21

J. C. Hubbs and G. M. Grosof

June 4, 1956

Printed for the U. S. Atomic Energy Commission

THE SPIN OF NEON-21*

J. C. Hubbs† and G. M. Grosof
Department of Physics, Columbia University, New York, New York

June 4, 1956

The spin of neon-21 has been shown to be 3/2 by the atomic beam magnetic resonance method utilizing the metastable $2p^5 - 3s\ ^3P_2$ state of neon. The assignment is made from a comparison of Zeeman frequencies in neon-20 and neon-21 at the same magnetic field.

INTRODUCTION

The spin and quadrupole moment of neon-21 are of particular interest because of the "anomalous" behavior of sodium-23 in a region where protons and neutrons are filling the d 5/2 level and should therefore, according to zero-order shell theory, result in spin 5/2. An explanation for the observed spin has been a $(d\ 5/2)^3$ configuration, but recent measurements[1,2] have shown a relatively large and positive quadrupole moment entirely out of line with such a quadrupole-free assignment. A series of experiments designed to obtain the spin, magnetic moment, and quadrupole moment of neon-21 has therefore been undertaken.

The investigation by members of the Columbia molecular and atomic beams laboratory of the metastable states of the rare gases--especially the work of Hughes and Weinreich[3] on helium-3--has provided a basis for the research. The principal problem, then, has been the extension of existing techniques two orders of magnitude farther in signal-to-noise ratio so that observations might be made on a single transition in neon-21. K. Clausius had kindly furnished us a 10-cc sample of neon enriched to 9.8% in neon-21.

---

*This research supported in part by the Office of Naval Research.

†Present address: University of California Radiation Laboratory, Berkeley, California.

[1] Perl, Rabi, and Senitzky, Phys. Rev. 98, 611 (1955).

[2] Sagalyn, Phys. Rev. 94, 885 (1954).

[3] V. W. Hughes and G. Weinreich, Phys. Rev. 95, 1451 (1954).

THEORY OF THE EXPERIMENT

The $^3P_2$ metastable state of neon is the lowest member of the configuration $2p^5 - 3s$, which defines the first excited states of neon. The lifetime of the state has been estimated to be more than 1 second in a field-free region. No known electric or magnetic fields utilized in this experiment could result in an enhancement by more than a factor of ten of the decay rate. Detection of the state is accomplished by observation of the electrons that are ejected from a metal surface by impinging metastables. The probability of this process is approximately 1/2.

An interpretation-free determination of the spin of neon-21 may be made from a comparison of the Zeeman frequencies in neon-20 and neon-21 at a magnetic field which is sufficiently low so that the magnetic energy of the atom is negligible in comparison with hyperfine structure intervals in neon-21. The effective g-value (g_F) for the interacting system of nucleus and electrons is then the product of the Landé g_J factor and the relative projection of the electronic angular momentum on the direction of total angular momentum, F. The ratio of Zeeman frequencies in neon-21 to that in neon-20, g_F/g_J, is then just the relative projection factor,

$$g_F/g_J = \frac{\langle \vec{J}\cdot\vec{F} \rangle}{\vec{F}^2} = \frac{F(F+1) + J(J+1) - I(I+1)}{2F(F+1)} .$$

APPARATUS

The apparatus, a modification of the system used by Hughes and Tucker,[3] is illustrated in Fig. 1. The gas system consists of several reservoirs for storing the 10-cc sample of enriched neon, a titanium metal cleaner operating at 750°-1000°C to remove hydrogen, oxygen, and nitrogen from the gas, the discharge tube,[4] and a mercury diffusion pump which backs the oil pumps on the can and returns the neon to the discharge tube at operating pressure. Approximately 1 cc of circulating gas is required to bring the discharge tube pressure to 0.3 mm hg. A Toeppler pump is used to return the gas to the reservoirs after conclusion of a run.

---

[4] Grosof and Hubbs, Rev. Sci. Instr. To be published.

Metastable atoms issue from a 0.003-by-0.7-cm slit in the wall of the discharge tube. The direct beam at the detector contains approximately 3×10^7 electrons per second liberated by high-energy photons issuing from the source and 2×10^6 electrons per second from metastable neon-20 atoms. Thus approximately 10^4 electrons per second are to be expected from a transition between two magnetic substates in neon-21.

The principal modification to the apparatus was the introduction of an ac detection scheme using an electron multiplier, a tuned amplifier at 30 c/s, and a lock-in detector having an output time constant from 10 seconds to 1 minute. The beam is chopped at a 30 c/s rate by pulsing the radio-frequency magnetic field. All combined sources of noise in the electronic system are smaller than the signal obtained from a transition in neon-21 by a factor of 10 or more. The signal-to-noise ratio obtained for Zeeman transitions in neon-20 by use of the flop-out system, which permits the direct beam to hit the detector, proved to be 7/1 as compared to the expected 1000/1 for statistical processes.

THE RESONANCE METHOD

A resonance method was sought which would combine the discrimination of the flop-in method against components of the beam that do not experience a change of state with the spectroscopic advantages of the flop-out system, particularly the applicability of the latter system to atoms with integral electronic angular momentum. Several possibilities have been considered: one for which the standard flop-out system is used but the central (refocused) beam is simply blocked and everything that experiences a change of state is captured by a large detector to the rear of the stop, the other a scheme which was adopted as follows (Fig. 2). The collimator is replaced by a half-plane stop, and an extended detector, also half-plane, is placed in the shadow of the collimator stop. For a refocused beam the points of intersection of any trajectory with the source, collimator, and detector plane defines a straight line. Thus a transition which results in a change of the high-field magnetic moment in one direction produces deflections toward the detector. The deflection so experienced is given by $\Delta m_J S_a E_o/E$, where $S_a = g_J u_o \, dH/dz \, L^2/4E_o$, so that the fraction of atoms that experience a deflection x or greater is given by

$$\rho(x) = \int_{\Delta m_J S_a E_o/x}^{\infty} E_o^{-2} \; E \exp(-E/E_o) dE = (1 + \Delta m_J S_a/x) \exp(-\Delta m_J S_a/x) .$$

The effective detector width is thus given by

$$\bar{X} = \int_0^{\infty} \rho(x)\, dx = S_a \Delta m_J .$$

Since the system throws away moment changes of one sign, a transition results in an intensity equivalent to the number of appropriate atoms in the direct beam $S_a \Delta m_J/2$ wide.

Application of this scheme to the apparatus led to a reduction of the background from photons and neon-20 by a factor of 30 to 40, and an improvement in the signal-to-noise ratio to a consistent 1/1 for a single-line transition in neon-21.

RESULTS

Zeeman resonances in neon-21 have been observed for magnetic fields between 1 and 10 gauss; a typical set of data is given in Fig. 3. The experimental data show values for the ratio of Zeeman frequencies in neon-21 to the resonance frequency of neon-20 of 0.57 ± 0.005, 0.63 ± 0.01, and 0.80 ± 0.04. Theoretical values of g_F/g_J for $J = 2$, $I = 3/2$, are 0.5714, 0.6285, 0.800, and 2.00 for Zeeman transitions in the states $F = 7/2$ through $F = 1/2$ respectively. The Zeeman resonance in the state $F = 1/2$ has not been observed.

In addition to these data a large number of transitions in the intermediate field region have been observed. Interpretation of the data is so equivocal, because of the very low signal-to-noise ratio and the presence of many multiple quantum transitions, that determination of the hyperfine structure intervals will have to await further improvements in the experimental technique.

ACKNOWLEDGMENTS

The authors wish to express their indebtedness to Prof. I. I. Rabi for the help and encouragement which he has extended during the course of the research and to Prof. P. Kusch for encouragement and stimulating discussion.

FIGURE CAPTIONS

Fig. 1. The modified atomic beam apparatus.

Fig. 2. Calibrator and detector arrangement for the resonance system. Refocused trajectories and trajectories for the appropriate moment change are shown.

Fig. 3A. Zeeman transitions in neon-21 for a magnetic field of 6.6 gauss.

Fig. 3B. Typical Zeeman transition in neon-20.

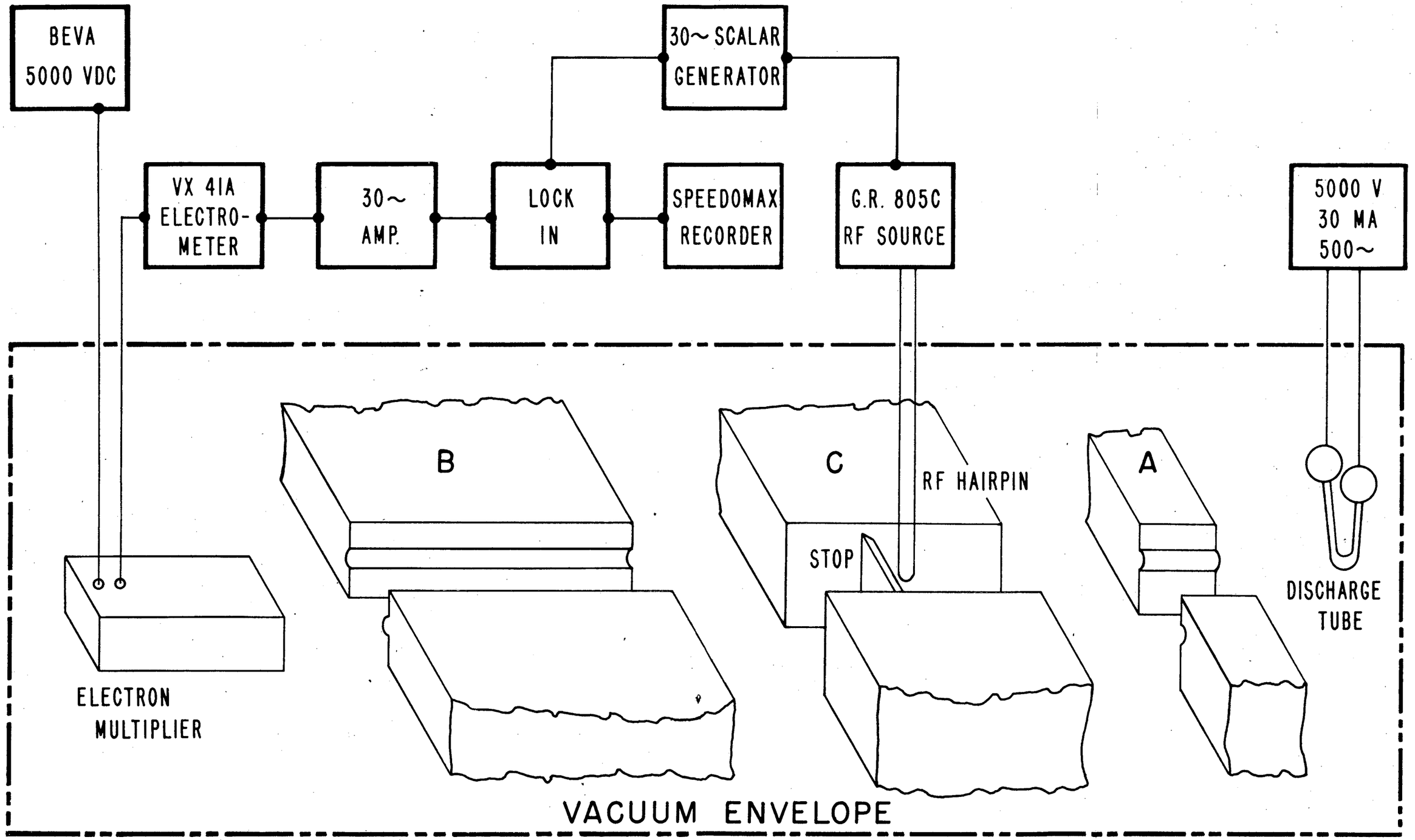
BEVA
5000 VDC
30~ SCALAR
GENERATOR
VX 41A
ELECTRO-
METER
30~
AMP.
LOCK
IN
SPEEDOMAX
RECORDER
G.R. 805C
RF SOURCE
5000 V
30 MA
500~
B
C
RF HAIRPIN
A
STOP
DISCHARGE
TUBE
ELECTRON
MULTIPLIER
VACUUM ENVELOPE

Fig. 1

24562-2

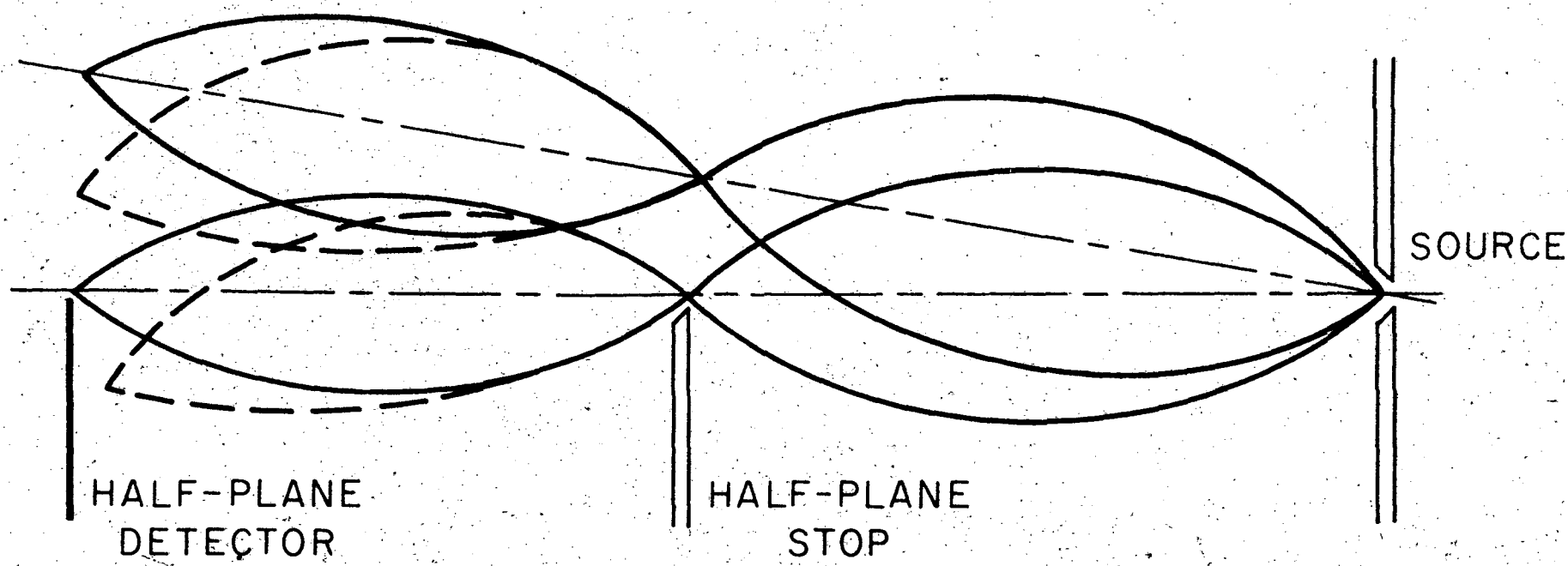

Fig. 2

24563-1

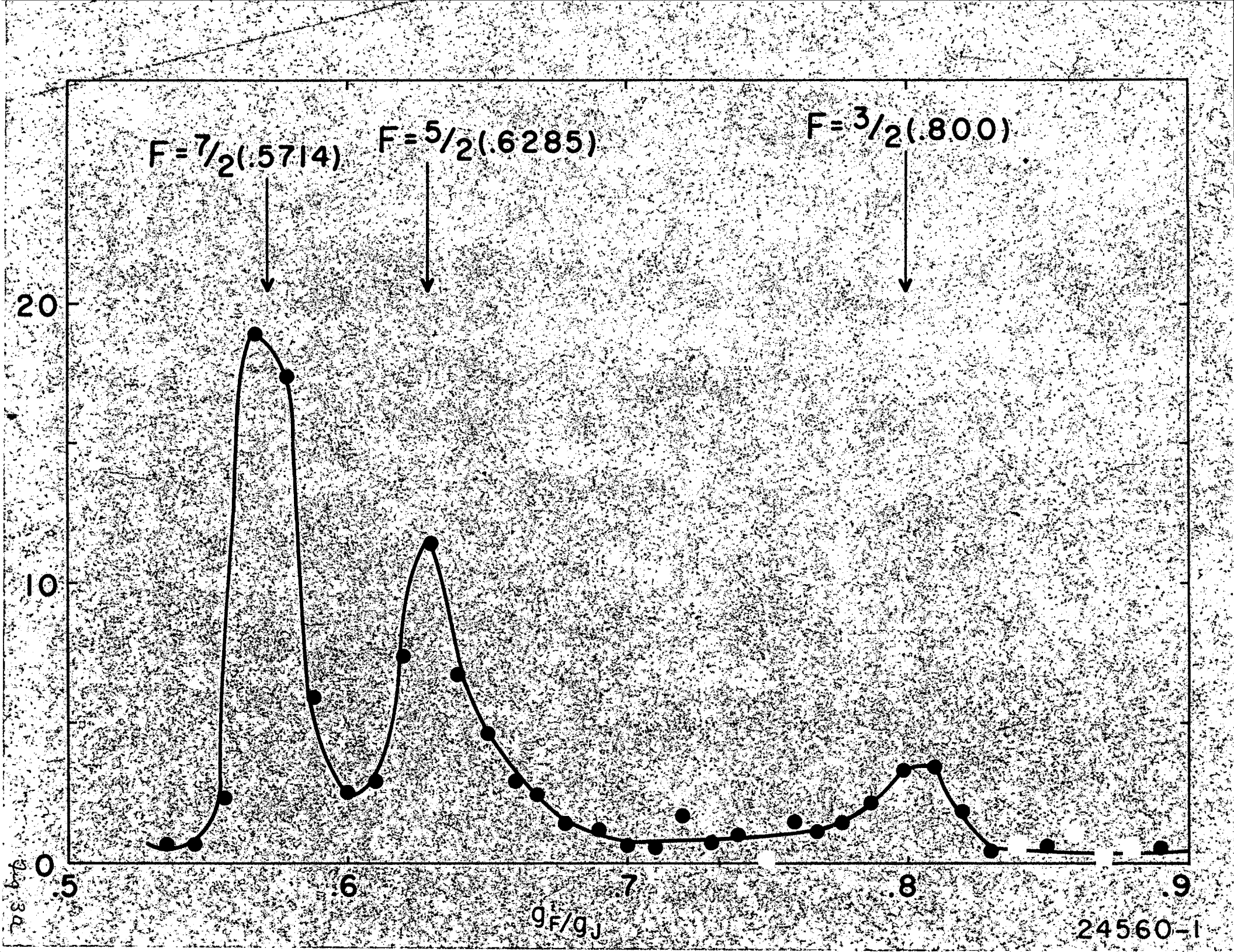

Fig. 3a

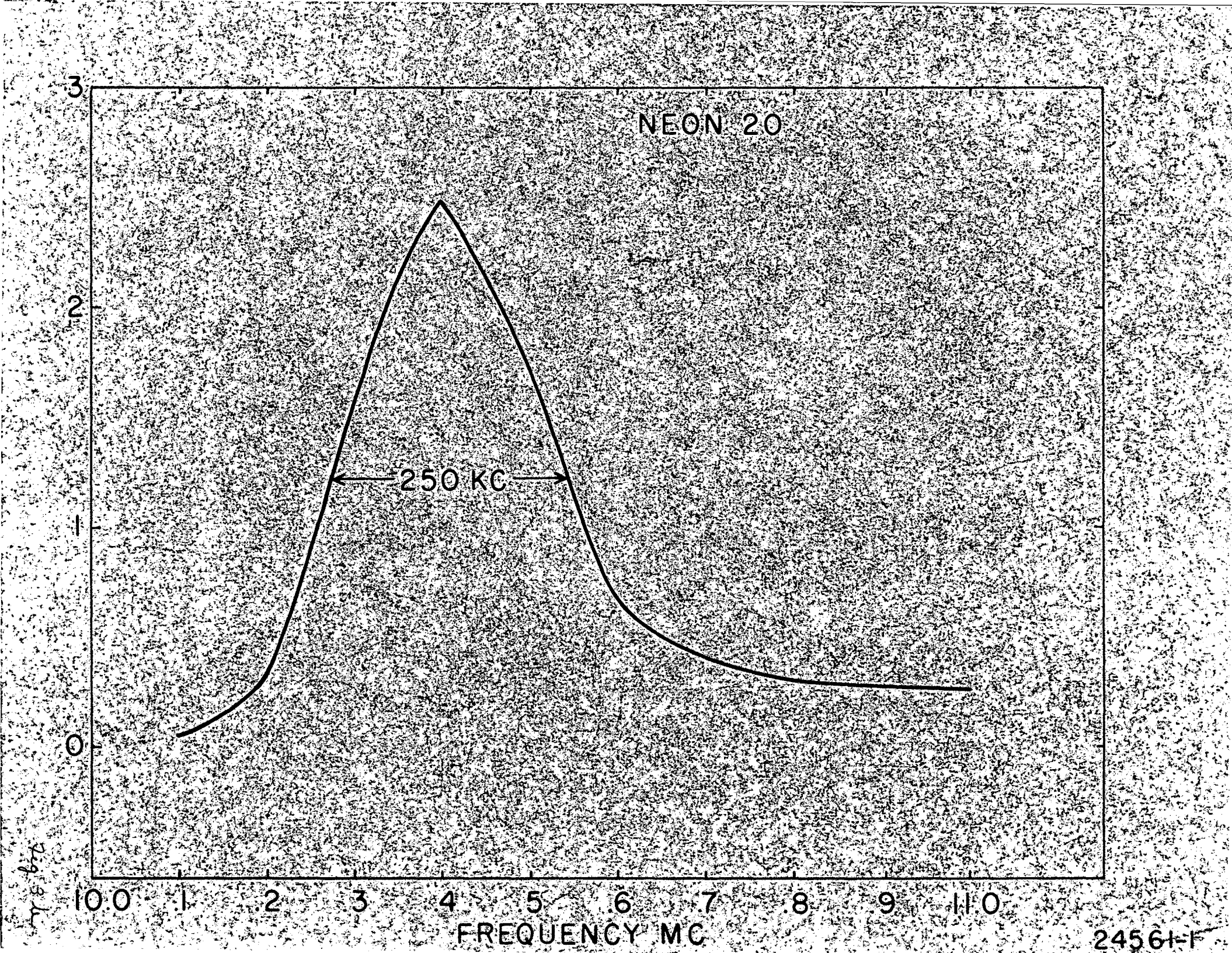

Fig 4